


Article

Effect of Powder Preparation Techniques on Microstructure, Mechanical Properties, and Wear Behaviors of Graphene-Reinforced Copper Matrix Composites

Doan Dinh Phuong^{1,*}, Pham Van Trinh^{1,2,*} , Phan Ngoc Minh², Alexandr A. Shtertser³ 
and Vladimir Y. Ulianitsky³

¹ Institute of Materials Science, Vietnam Academy of Science and Technology, Hanoi 10072, Vietnam

² Graduate University of Science and Technology, Vietnam Academy of Science and Technology, Hanoi 10072, Vietnam

³ Lavrentyev Institute of Hydrodynamics SB RAS, Lavrentyev Ave. 15, Novosibirsk 630090, Russia

* Correspondence: phuongdd@ims.vast.ac.vn (D.D.P.); trinhpv@ims.vast.vn (P.V.T.); Tel.: +84-943190301 (P.V.T.)

Abstract: In this study, the effect of powder preparation techniques on microstructure, mechanical properties, and wear behaviors of graphene-reinforced copper matrix (Gr/Cu) composites was investigated. The composite powders were prepared by two different techniques including high-energy ball (HEB) milling and nanoscale dispersion (ND). The obtained results showed that the ND technique allows the preparation of the composite powder with a smaller and more uniform grain size compared to the HEB technique. By adding Gr, the mechanical properties and wear resistance of the composite were much improved compared to pure Cu. In addition, the composite using the powder prepared by the ND technique exhibits the best performance with the improvement in hardness (40%), tensile strength (66%) and wear resistance (38%) compared to pure Cu. This results from the uniform grain size of the Cu matrix and the good bonding between Cu matrix and Gr. The strengthening mechanisms were also analyzed to clarify the contribution of the powder preparation techniques on the load transfer strengthening mechanisms of the prepared composite.

Keywords: Cu composite; graphene; microstructure; mechanical properties; wear behavior



Citation: Phuong, D.D.; Van Trinh, P.; Minh, P.N.; Shtertser, A.A.; Ulianitsky, V.Y. Effect of Powder Preparation Techniques on Microstructure, Mechanical Properties, and Wear Behaviors of Graphene-Reinforced Copper Matrix Composites. *Crystals* **2024**, *14*, 1000. <https://doi.org/10.3390/cryst14111000>

Academic Editor: Jan Macutkevicius

Received: 18 October 2024

Revised: 12 November 2024

Accepted: 13 November 2024

Published: 19 November 2024



Copyright: © 2024 by the authors. Licensee MDPI, Basel, Switzerland. This article is an open access article distributed under the terms and conditions of the Creative Commons Attribution (CC BY) license (<https://creativecommons.org/licenses/by/4.0/>).

1. Introduction

Copper matrix composites (CMCs) have wide applications in many different sectors, including aerospace, energy, and electronics, owing to their superior electrical conductivity, thermal conductivity, and mechanical qualities [1–3]. Nonetheless, the inadequate mechanical characteristics and wear resistance of copper matrix composites may lead to considerable damage and may diminish their operational lifespan. Consequently, enhancing their mechanical characteristics and resistance to friction and wear is crucial for practical applications. The addition of reinforcement as a second phase is expected to enhance the performance of CMCs. Nevertheless, the electrical and thermal conductivity are significantly compromised. Conversely, carbon nanofibers (CNFs) and carbon nanotubes (CNTs) have emerged as appealing reinforcements for CMCs [4–8]. Nevertheless, inadequate wettability between CNFs and copper results in suboptimal mechanical characteristics. The uniform dispersion of CNTs in CMCs is challenging, impeding their application. Graphene has recently been extensively studied as a reinforcement for CMCs [9,10]. Owing to its unique two-dimensional structure, graphene exhibits superior electrical conductivity, thermal conductivity, and mechanical characteristics [11,12]. Consequently, graphene-CMCs may exhibit not only superior mechanical qualities and wear resistance but also satisfactory electrical and thermal characteristics. Presently, powder metallurgy, molecular-level mixing, and electrochemical deposition are standard techniques for the preparation of

graphene-CMCs [13–15]. Graphene, in either powdered form or as a dispersion in liquid, is frequently utilized as a raw element in these methodologies. Nonetheless, the van der Waals forces between the aromatic rings frequently lead to the agglomeration of graphene in the CMCs, presenting a significant difficulty in achieving high-performance graphene-CMCs [13,16–19]. Furthermore, the integrity of the graphene structure may be compromised throughout the rigorous process, resulting in a suboptimal performance. Therefore, there is an urgent necessity to devise novel preparation procedures for graphene-CMCs to enhance the dispersibility and integrity of graphene. The microstructures of copper matrices significantly influence their mechanical properties. Nanograins, textures, twins, and heterogeneous structures have demonstrated advantages for the mechanical characteristics and wear resistance of the material. Ultrafine structures, consisting of two unique grain sizes, are characteristic heterogeneous structures that substantially influence the mechanical properties of materials [16,17,20–22].

Thus, the goal of this study was to evaluate the influence of the initial composite powder preparation method on the properties of the Gr/Cu composites after sintering. The composite powders were prepared by using two different techniques including high-energy ball (HEB) milling and nanoscale dispersion (ND). The microstructure, mechanical properties, and wear behaviors of the prepared composite were investigated and presented.

2. Materials and Methods

2.1. Preparation of Gr/Cu Composites

Preparation of Gr/Cu powder: Gr/Cu powders containing 2 vol.% Gr was prepared by using two different approaches including high-energy ball milling (HEB-Approach 1) and nanoscale dispersion (ND, Approach 2) as shown in Figure 1.

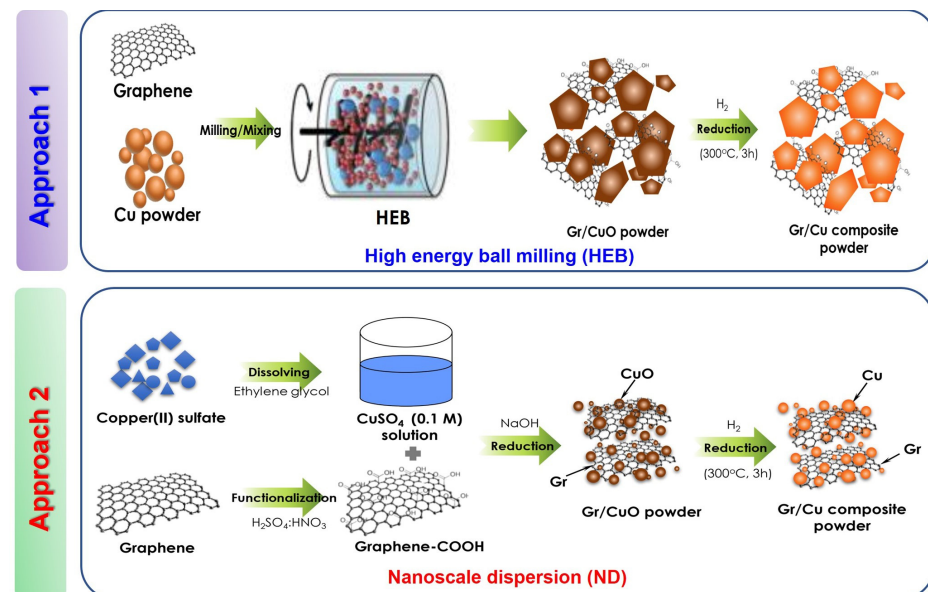


Figure 1. Schematic view of the preparation process for Gr/Cu powder by using high energy ball milling (HEB-Approach 1) and nanoscale dispersion (ND, Approach 2).

+Approach 1: Firstly, the Gr (Figure 2a) powder was functionalized with a mixture of acids consisting of H_2SO_4 and HNO_3 ($v:v/3:1$) at a temperature of $70\text{ }^\circ\text{C}$ for 5 h. After that, the obtained solution was filtered and washed with alcohol and distilled water to obtain the Gr-COOH. The obtained Gr-COOH was then dispersed in alcohol to form a Gr-COOH solution with a concentration of 1 g/1 L. The mixture of Cu powder (Figure 2b) and Gr-COOH powders is milled and mixed by high-energy ball (HEB) milling with a speed of 200 rpm and a ball/powder ratio of 10:1. The obtained Gr/Cu powder after milling was reduced in H_2 at a temperature of $300\text{ }^\circ\text{C}$ for 3 h to remove metal oxide components to obtain Gr/Cu powder.

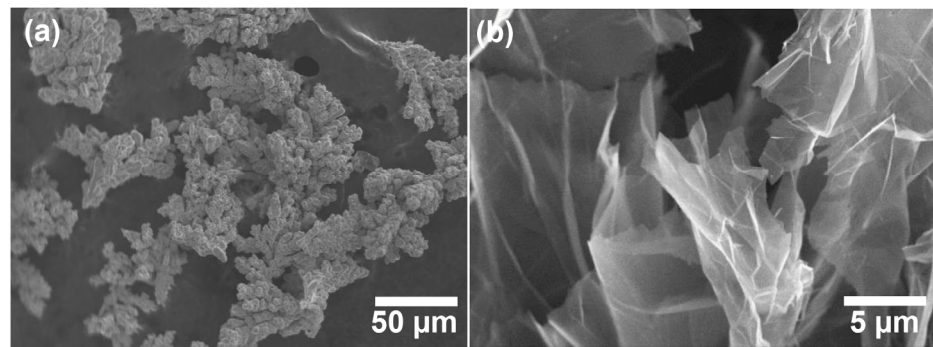


Figure 2. SEM images of (a) Cu powder and (b) graphene powders.

+Approach 2: The preparation process of composite powder by using ND technique is described in Figure 1. Firstly, the functionalized Gr was dispersed in alcohol to form Gr-COOH solution with concentration of 1 g/1 L. Then, the mixture of CuSO_4 salt and Gr-COOH is stirred together by magnetic stirrer at speed of 500 rpm for 1 h. Next, NaOH solution is slowly added to the above solution. After that, the obtained solutions were filtered, washed, and dried at 300 °C to obtain Gr/CuO powder. The Gr/CuO powder was then reduced in H_2 at temperature of 280 °C for 3 h to remove metal oxide components to obtain Gr/Cu powder.

Sintering process: The sintering process of Gr/Cu composite material is described in Figure 3. Hot isostatic pressing (AIP6-30 H, American Isostatic Presses Inc., Columbus, OH, USA) were used to consolidate the Gr/Cu composite specimens. Firstly, the prepared Gr/Cu powder was pre-compacted to form bar-shaped samples with dimensions of 40 × 10 × 3 mm. The specimens were then put in the chamber and heated (5 °C/min) up to 500 °C and held for a 30 min dwell time, followed by increasing the temperature to 900 °C (10 °C/min) and applying the pressing process under a load of 100 MPa for 120 min to obtain Gr/Cu composite.

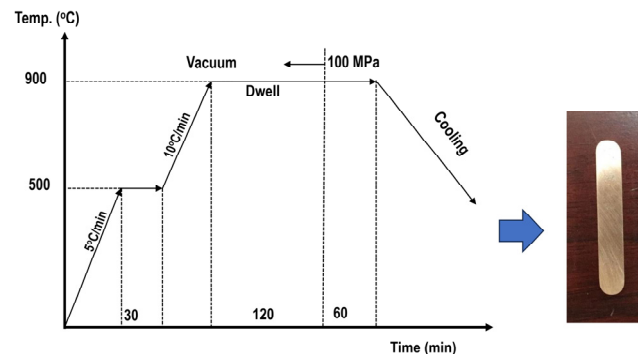


Figure 3. Sintering process of Gr/Cu composite by hot isostatic pressing technique.

2.2. Characterizations

The microstructure was observed by a scanning electron microscope (SEM) (Hitachi S4800, Tokyo, Japan), SEM energy dispersive spectroscopy (SEM-EDS, Hitachi S-4800, Tokyo, Japan), and JEOL JSM-6500F equipped with an electron backscatter diffraction (EBSD) detector. An X-ray diffraction (XRD) analysis was recorded by using an X-ray diffractometer (Bruker D8 Endeavor, Billerica, MA, USA) with $\text{CuK}\alpha$ radiation. The Archimedes method was used to determine the experimental density of sintered composites. Hardness was assessed with a Vickers hardness tester (Mitutoyo HM-124) with a load of 9.8 N for a duration of 10 s. Tensile characteristics were assessed utilizing a universal testing equipment (INSTRON 8848 micro-tester) at a cross-head velocity of 0.2 mm/min at ambient temperature. A ball-on-disc apparatus (CMS tribometer) was employed for the wear test, utilizing steel balls under a load of 10 N, at a speed of 5 cm/s, and a sliding distance of 10 m.

3. Results

3.1. Microstructure

The microstructure of composite powders prepared by different dispersion techniques is shown in Figure 4. Figure 4a is a Gr/Cu powder prepared by the HEB technique. As observed in the figure, Gr is dispersed on the surface of deformed Cu particles during the milling process. However, the appearance of Gr clusters is also observed in the Cu matrix. This indicated that the HEB technique is less effective in dispersing Gr. Figure 4b shows the morphology of Gr/Cu powder prepared by the ND technique. The obtained results showed the ability to evenly disperse Gr and Cu particles during the preparation process. This is attributed to the formation of Cu nanoparticles on the surface of Gr sheets. The Gr sheets are surface modified with COOH functional groups at the boundary. These functional groups will interact with Cu^{2+} ions. Then, the chemical reduction process is carried out and Cu nanoparticles are formed at the positions of the functional groups. This process helps to disperse Cu particles more uniformly than the HEB technique. The presence of Gr in the powder was confirmed by EDS spectra at position B for the powder prepared by the HEB technique and position D for the powder prepared by the ND technique.

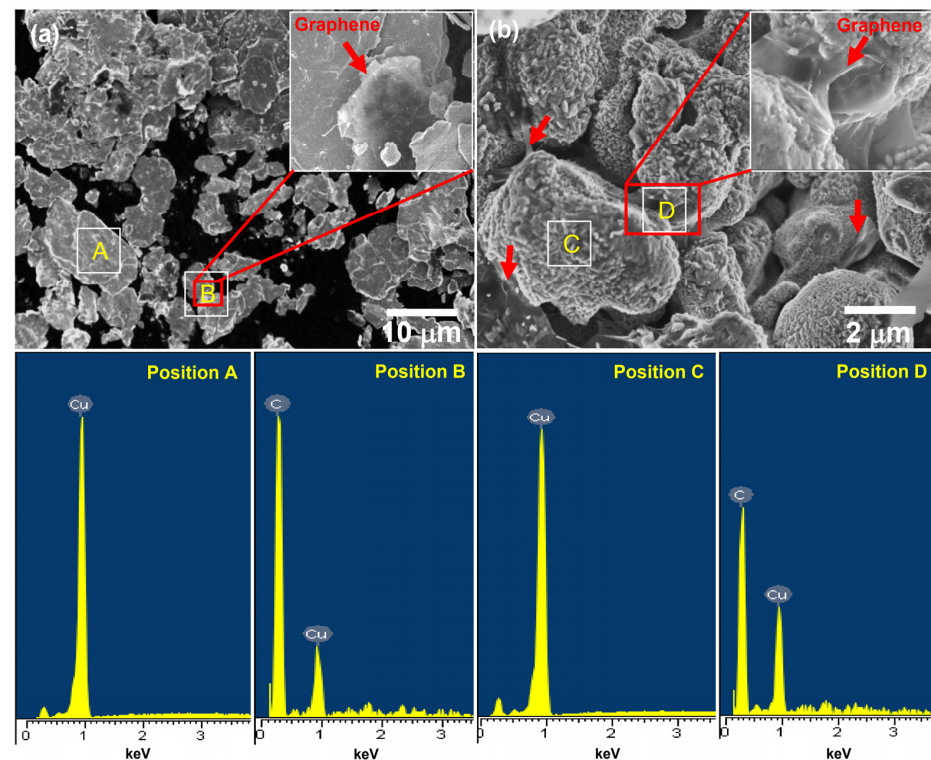


Figure 4. SEM images and EDS spectra of Gr/Cu powder prepared by using different techniques (a) HEB and (b) ND.

To observe the distribution of Gr in the Cu matrix, the composites were polished and etched with the etchant containing 25 mL H_2O + 25 mL NH_4OH + 5 mL H_2O_2 for 15 s at room temperature. Figure 5 shows the distribution of Gr in the Cu matrix. As can be seen, the presence of some Gr clusters was observed with the composite using the powder prepared by HEB (Figure 5a). Meanwhile, the uniform dispersion of Gr was obtained with the composite using the powder prepared by the ND technique (Figure 5b). This is consistent with the SEM observation with the prepared powder. Consequently, the uniform dispersion of Gr in the Cu matrix could be obtained by using the ND technique.

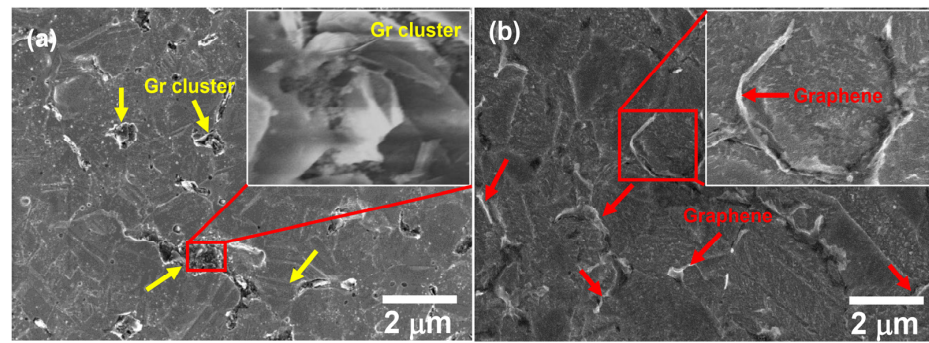


Figure 5. SEM images of Gr/Cu composite using powder prepared by using different techniques: (a) HEB and (b) ND.

Figure 6 shows the grains of pure Cu and Gr/Cu composites with powder prepared by different techniques. As can be seen, the preparation techniques strongly affected the microstructure of the sintered samples. The samples using the powder prepared by the HEB technique exhibited an ununiform grain size. In contrary, uniform grain sizes were obtained with the samples using the powder prepared by the ND technique. In addition, the grain size of samples with the prepared by ND technique is smaller than that of the sample using the powder prepared by the HEB technique. Consequently, the ND technique facilitates the preparation of powder samples with uniformly dispersed Gr and produces materials with a more consistent ultrafine particle size compared to the HEB technique.

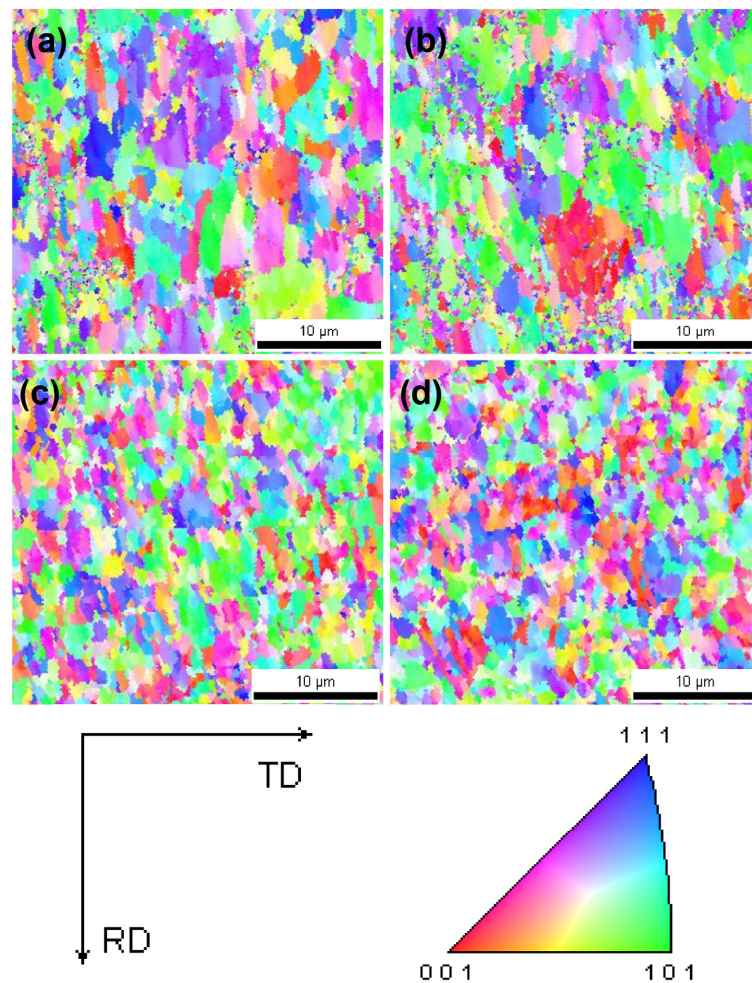


Figure 6. EBSD inverse pole figure (IPF) maps of (a) pure Cu (HEB), (b) Gr/Cu (HEB), (c) pure Cu (ND), and (d) Gr/Cu (ND).

Figure 7a shows the X-ray diffraction patterns for pure Cu and Gr/Cu composites. The XRD patterns of the samples reveal only Cu diffraction peaks at $2\theta = 43.29^\circ$, 50.43° , 74.13° , 89.93° , and 95.14° corresponding to (111), (200), (220), (311), and (222) planes, respectively. There are no typical peaks of the CuO phases detected. This demonstrated that no oxidation phase was formed during the preparation process. In addition, the typical peak of Gr located at 26.3° has not been identified in the composites. This could be due to the concentration of Gr in the prepared composites being too small to be detected [23,24]. The crystallite size of Cu was calculated by using Scherrer's equation:

$$D = \frac{0.9\lambda}{\beta \cos(\theta)}$$

where D is the crystallite size, $\lambda = 0.15406$ nm is the wavelength of X ray source, β is the full width at half maximum (FWHM) calculated from XRD profiles, and θ is the peak position. Figure 7b shows the crystallite size of the pure Cu and Gr/Cu composites. As can be seen, the crystallite size of the samples (both the pure Cu and Gr/Cu composites) prepared by the ND technique is smaller than that of the samples prepared by the HEB technique.

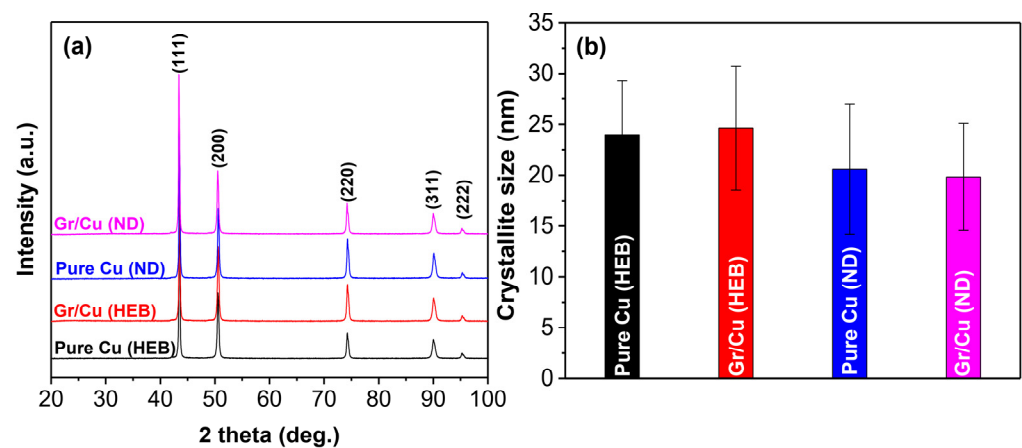


Figure 7. (a) XRD patterns and (b) crystallite size of pure Cu and Gr/Cu with powder prepared by HEB and ND techniques.

3.2. Mechanical Properties

Measurements of density, hardness, and tensile strength were carried out to study the influence of the initial Gr/Cu powder preparation technique on the composite properties. As shown in Table 1, the density of the composites decreased with the addition of Gr. The hardness of Gr/Cu composites with powder samples prepared by the different methods is shown in Figure 8a. The results show that after coagulation, the hardness of the material with powder samples prepared by HEB increased by 29%. However, the hardness of the composite using the powder prepared by the ND technique increased by 40%. Similarly, the tensile strength of the composite with powder samples prepared by the ND technique also showed significant improvement compared to the HEB technique. The tensile strength of the composite with powder samples prepared by HEB technique increased by 29%, while for samples prepared by the ND technique, the tensile strength increased by 66% (Figure 8b). The increase in mechanical properties of composites with powder samples prepared by ND technique is attributed to the uniform dispersion of Gr in the Cu matrix and the strong bonding between Gr and Cu matrix during the fabrication process. In addition, the smaller grain size of the composites using the powder prepared by ND, as presented in the previous section, also contributed to the enhancement on the mechanical properties.

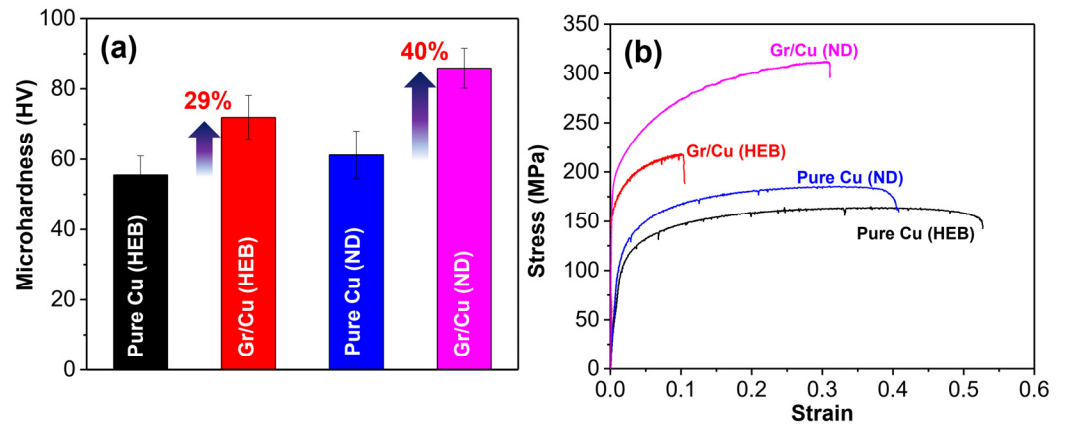


Figure 8. (a) Microhardness and (b) tensile strength of pure Cu and Gr/Cu with powder prepared by HEB and ND techniques.

Table 1. Relative density, hardness, and tensile strength of pure Cu and Gr/Cu composites with powder prepared by different dispersion techniques.

Composite	Relative Density (%)	Microhardness (HV)	σ_{YS} (MPa)	σ_{UTS} (MPa)	Elongation (%)
Pure Cu (HEB)	98.1 ± 1.2	55.5 ± 5.4	120 ± 9.4	168 ± 10.5	55 ± 3.1
Gr/Cu (HEB)	97.6 ± 1.4	71.9 ± 6.2	188 ± 11.2	218 ± 12.8	11 ± 4.5
Pure Cu (ND)	98.5 ± 1.1	61.2 ± 6.8	137 ± 7.8	187 ± 9.9	42 ± 3.4
Gr/Cu (ND)	97.8 ± 1.3	85.9 ± 5.7	248 ± 8.9	311 ± 10.7	30 ± 2.8

To evaluate the ability to enhance the mechanical properties of materials, the mechanisms of enhancing the mechanical properties of materials such as the Hall–Petch, Orowan strengthening, dislocation density, and load transfer are considered and evaluated.

The $\Delta\sigma_{gb}$ is calculated by using the Hall–Petch equations as follows [25]:

$$\sigma_y = \sigma_0 + k_y d^{-1/2} \quad (1)$$

$$\Delta\sigma_{gb} = k_y (d_1^{-1/2} - d_2^{-1/2}) \quad (2)$$

where $k_y = 0.14 \text{ MPa}/\text{m}^{1/2}$ is the Hall–Petch coefficient for pure Cu [26], and d is the grain size of the Cu matrix.

The $\Delta\sigma_{dis}$ is contributed by the thermal mismatch between Gr and Cu matrix at the interface and described as shown in the following equation [27]:

$$\Delta\sigma_{TM} = \alpha G_m b \sqrt{\frac{12\Delta T \Delta CTE V_{Gr}}{bd}} \quad (3)$$

where α (≈ 1.25), G_m ($\approx 42.1 \text{ GPa}$), and b (≈ 0.256) are the dislocation strengthening efficiency, the shear modulus, and the Burgers vector of the matrix [26]; ΔT ($\approx 680 \text{ K}$) is defined as a difference between the fabrication and testing temperatures; and ΔCTE is the difference in CTE between the Cu matrix ($17 \times 10^{-6} \text{ K}$) and Gr ($-2 \times 10^{-6} \text{ K}$) [28].

The $\Delta\sigma_{Orowan}$ value is usually contributed by the strengthening of nano-sized reinforcements in a matrix by inhibiting the dislocation motions to form Orowan loops during plastic deformation. The $\Delta\sigma_{Orowan}$ value can be estimated by the following equation [29].

$$\Delta\sigma_{Orowan} = \frac{0.13 G_m b}{\lambda} \ln \frac{r}{b} \quad (4)$$

where d_p is the average flake size of graphene, r is defined as $d_p/2$, and λ is an interparticle spacing and is defined as shown in Equation (5).

$$\lambda \approx d_p \left[\left(\frac{1}{2VGr} \right)^{1/3} - 1 \right] \quad (5)$$

The modified shear-lag model is employed to estimate the load transfer strengthening, which is described by the following equation [30].

$$\sigma_{cy} \approx \sigma_{my}^* V_{Gr} \left[1 + \frac{(l+t)S}{4l} \right] + \sigma_{my}^* (1 - V_{Gr}) \quad (6)$$

where σ_{my}^* is the yield strength of matrix ($=\sigma_{my} + \Delta\sigma_{gb} + \Delta\sigma_{dis}$). The values l , t , and S are the sizes of particles parallel and perpendicular to the loading direction, and S is the aspect ratio of the particle.

Table 2 presents the calculated the contribution of strengthening mechanisms to the yield strength of pure Cu and Gr/Cu composites with powder prepared by using different dispersion techniques. Figure 9 shows the contribution of the strengthening mechanisms to the yield strength of composite materials with powder samples prepared by HEB technique. As can be seen, the contribution of the strengthening mechanisms, the majority of the contribution comes from the load transfer mechanism, which is nearly 60%. Meanwhile, with powder samples prepared by the ND technique, the contribution of the load transfer mechanism is up to more than 70% (Figure 10). As a result, the ND technique allows the fabrication of composite materials with higher mechanical strength than the HEB technique due to the uniform dispersion of Gr and the high interface bond strength between Gr and the Cu matrix.

Table 2. Contribution of strengthening mechanisms to the yield strength of pure Cu and Gr/Cu composites with powder prepared by using different dispersion techniques.

Composite	Measured Y. S. (MPa)	Calculated Enhancement in Y. S. (MPa)			
		Grain Boundary Strengthening	Dislocation Strengthening by CTE Mismatch	Orowan Strengthening	Load Transfer
Pure Cu (HEB)	120	-	-	-	-
Gr/Cu (HEB)	188	10.5	16.2	1.1	40.2
Pure Cu (ND)	137	-	-	-	-
Gr/Cu/ND)	248	14.9	16.2	1.1	78.8

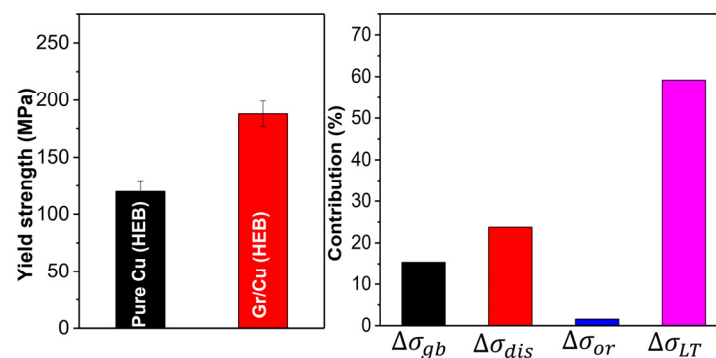


Figure 9. Contribution of strengthening mechanisms to the yield strength of Gr/Cu composites with powder prepared by HEB technique.

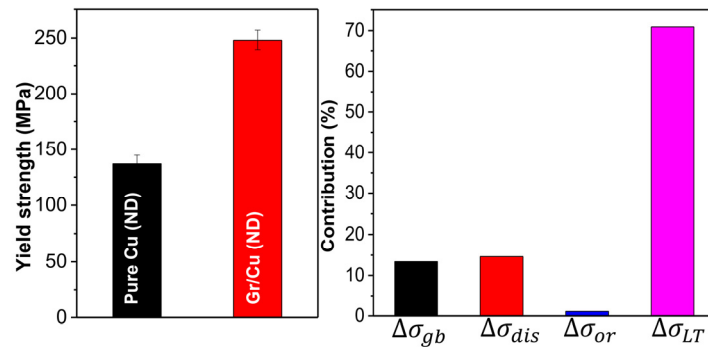


Figure 10. Contribution of strengthening mechanisms to the yield strength of Gr/Cu composites with powder prepared by ND technique.

3.3. Wear Behaviors

The friction coefficient of the Gr/Cu composite with powder prepared by different techniques is shown in Figure 11a,b. From Figure 11, it can be seen that the friction coefficient of the material after being reinforced with Gr decreased. With the sample prepared by the HEB technique, the friction coefficient of the composite decreased by 34%, while the friction coefficient of the sample prepared by the ND technique decreased by 43%. Figure 11c is a graph showing the wear rate of the composite prepared with powder samples prepared by different techniques. Similarly to the friction coefficient of the samples, the wear rate of the composite prepared by the ND technique was more effective, decreasing by 38% compared to the composite prepared with powder prepared by the HEB technique (27%).

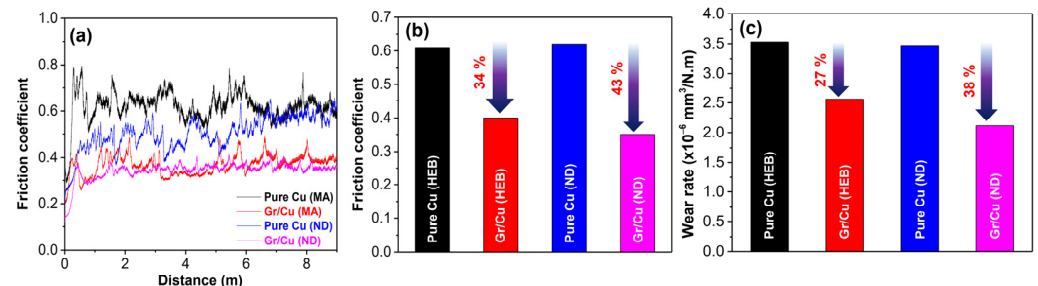


Figure 11. (a,b) Friction coefficient and (c) wear rate of pure Cu and Gr/Cu with powder prepared by HEB and ND techniques.

It is well known that graphene exhibits a variety of beneficial features that render it exceptionally effective in enhancing wear resistance and diminishing the wear rate of metal matrix composites. The integration of graphene into the copper matrix considerably enhances stress dispersion and mitigates stress concentration. In pure copper, the stress regions caused by applied loads will be more profound and susceptible to localized stress concentrations and fracturing. The incorporation of graphene sheets in the composite facilitates the absorption and distribution of stress from applied loads, hence significantly reducing localized stress concentration. In addition, the spatial distribution of graphene significantly influences the wear resistance of the composite. The graphene in the composite serves to provide lubrication and inhibits interfacial delamination caused by weaker interlayer sliding. Finally, the distribution of graphene on the composite surface serves as a barrier, effectively inhibiting abrasive particles from penetrating the thin foil surface. The hardness of abrasive particles may exceed that of the re-crystallized regions of pure copper, leading to the penetration of these particles into the copper surface during sliding, resulting in more pronounced wear tracks. The barrier effect of graphene markedly diminishes the abrasion depth of the composite and efficiently inhibits delamination and spalling. Moreover, abraded graphene sheets can offer enhanced lubrication, which is crucial for efficiently reducing the friction coefficient and preventing excessive wear.

In conclusion, graphene promotes advantageous characteristics, such as improved lubrication, stress spread, and the inhibition of delamination and spalling. This effectively reduces the wear rate of the composite and enhances its wear resistance.

4. Conclusions

We have investigated the effect of powder preparation techniques on the microstructure, mechanical properties, and wear behaviors of Gr/Cu composites. The obtained results demonstrated that the mechanical properties and wear resistance of the composite could be improved with the addition of Gr. This is attributed to Gr promoting advantageous characteristics including self-lubrication, stress dissipation, and the inhibition of delamination and spalling. In comparison to pure Cu, the hardness of the Gr/Cu composite is elevated by 40%, the average friction coefficient is reduced by 43%, and the tensile strength of the composite is enhanced to 311 MPa with an elongation of 30%. This work is expected to offer insights into the industrial production of high-performance Gr/Cu composites.

Author Contributions: Conceptualization, P.V.T., P.N.M. and D.D.P.; validation, D.D.P. and P.V.T.; formal analysis, P.V.T.; investigation, D.D.P. and P.V.T.; writing—original draft preparation, P.V.T.; writing—review and editing, P.V.T. and D.D.P.; supervision, P.N.M. and D.D.P.; project administration, P.V.T., A.A.S. and V.Y.U.; funding acquisition, P.V.T. and A.A.S. All authors have read and agreed to the published version of the manuscript.

Funding: This research was funded by Vietnam Academy of Science under grant number KHCBVL.01/22-23. The Russian authors thanks to the support from the Russian Foundation for Basic Research under project 20-53-54001.

Data Availability Statement: Data can be made available upon request.

Conflicts of Interest: The authors declare no conflicts of interest.

References

1. Madhesh, D.; Jagatheesan, K.; Sathish, T.; Balamaniandasuthan, K. Microstructural and Mechanical Properties of Copper Matrix Composites. *Mater. Today Proc.* **2021**, *37*, 1437–1441. [\[CrossRef\]](#)
2. Jamwal, A.; Mittal, P.; Agrawal, R.; Gupta, S.; Kumar, D.; Sadasivuni, K.K.; Gupta, P. Towards Sustainable Copper Matrix Composites: Manufacturing Routes with Structural, Mechanical, Electrical and Corrosion Behaviour. *J. Compos. Mater.* **2020**, *54*, 2635–2649. [\[CrossRef\]](#)
3. Luo, H.; Bao, R.; Ma, R.; Liu, J.; Nie, Y.; Yi, J. Preparation and Properties of Copper Matrix Composites Synergistically Strengthened by Al₂O₃ and CPD. *Diam. Relat. Mater.* **2022**, *124*, 108916. [\[CrossRef\]](#)
4. Sivasubramaniyam, V.; Ramasamy, S.; Venkatraman, M.; Gatto, G.; Kumar, A. Carbon Nanotubes as an Alternative to Copper Wires in Electrical Machines: A Review. *Energies* **2023**, *16*, 3665. [\[CrossRef\]](#)
5. Carneiro, Í.; Monteiro, B.; Ribeiro, B.; Fernandes, J.V.; Simões, S. Production and Characterization of Cu/CNT Nanocomposites. *Appl. Sci.* **2023**, *13*, 3378. [\[CrossRef\]](#)
6. Ya, B.; Xu, Y.; Meng, L.; Zhou, B.; Zhao, J.; Chen, X.; Zhang, X. Fabrication of Copper Matrix Composites Reinforced with Carbon Nanotubes Using an Innovational Self-Reduction Molecular-Level-Mixing Method. *Materials* **2022**, *15*, 6488. [\[CrossRef\]](#)
7. Štefanik, P.; Šebo, P. Thermal Expansion of Copper-Carbon Fiber Composites. *Theor. Appl. Fract. Mech.* **1994**, *20*, 41–45. [\[CrossRef\]](#)
8. Šebo, P.; Štefanik, P. Copper Matrix–Carbon Fibre Composites. *Int. J. Mater. Prod. Technol.* **2003**, *18*, 141–159. [\[CrossRef\]](#)
9. Hidalgo-Manrique, P.; Lei, X.; Xu, R.; Zhou, M.; Kinloch, I.A.; Young, R.J. Copper/Graphene Composites: A Review. *J. Mater. Sci.* **2019**, *54*, 12236–12289. [\[CrossRef\]](#)
10. Ali, S.; Ahmad, F.; Yusoff, P.S.M.M.; Muhamad, N.; Oñate, E.; Raza, M.R.; Malik, K. A Review of Graphene Reinforced Cu Matrix Composites for Thermal Management of Smart Electronics. *Compos. Part A Appl. Sci. Manuf.* **2021**, *144*, 106357. [\[CrossRef\]](#)
11. Yusaf, T.; Mahamude, A.S.F.; Farhana, K.; Harun, W.S.W.; Kadirgama, K.; Ramasamy, D.; Kamarulzaman, M.K.; Subramonian, S.; Hall, S.; Dhahad, H.A. A Comprehensive Review on Graphene Nanoparticles: Preparation, Properties, and Applications. *Sustainability* **2022**, *14*, 12336. [\[CrossRef\]](#)
12. Mbayachi, V.B.; Ndayiragije, E.; Sammani, T.; Taj, S.; Mbuta, E.R.; ullah khan, A. Graphene Synthesis, Characterization and Its Applications: A Review. *Results Chem.* **2021**, *3*, 100163. [\[CrossRef\]](#)
13. Shi, Z.; Sheng, J.; Liu, Z.; Yang, Z.; Xing, C.; Li, J.; Chen, W.; Wang, M.; Wang, L.; Fei, W. Graphene-like Carbon Nanosheet/Copper Composite with Combined Performance Designed by Pyrolyzing Trimesic Acid@copper Formate. *J. Mater. Res. Technol.* **2021**, *13*, 111–120. [\[CrossRef\]](#)
14. Li, X.; Miu, J.; An, M.; Mei, J.; Zheng, F.; Jiang, J.; Wang, H.; Huang, Y.; Li, Q. Preparation of Graphene/Copper Composites with a Thiophenol Molecular Junction for Thermal Conduction Application. *New J. Chem.* **2022**, *46*, 10107–10116. [\[CrossRef\]](#)

15. Chen, F.; Mei, Q.S.; Li, J.Y.; Li, C.L.; Wan, L.; Zhang, G.D.; Mei, X.M.; Chen, Z.H.; Xu, T.; Wang, Y.C. Fabrication of Graphene/Copper Nanocomposites via in-Situ Delamination of Graphite in Copper by Accumulative Roll-Compositing. *Compos. B Eng.* **2021**, *216*, 108850. [[CrossRef](#)]
16. Li, T.; Wang, Y.; Yang, M.; Hou, H.; Wu, S. High Strength and Conductivity Copper/Graphene Composites Prepared by Severe Plastic Deformation of Graphene Coated Copper Powder. *Mater. Sci. Eng. A* **2021**, *826*, 141983. [[CrossRef](#)]
17. Avcu, E.; Cao, H.; Zhang, X.; Guo, Y.; Withers, P.J.; Li, X.; Wang, N.; Yan, S.; Xiao, P. The Effect of Reduced Graphene Oxide Content on the Microstructural and Mechanical Properties of Copper Metal Matrix Composites. *Mater. Sci. Eng. A* **2022**, *856*, 143921. [[CrossRef](#)]
18. Choi, J.; Okimura, N.; Yamada, T.; Hirata, Y.; Ohtake, N.; Akasaka, H. Deposition of Graphene–Copper Composite Film by Cold Spray from Particles with Graphene Grown on Copper Particles. *Diam. Relat. Mater.* **2021**, *116*, 108384. [[CrossRef](#)]
19. Wang, M.; Zuo, T.; Xue, J.; Ru, Y.; Wu, Y.; Xu, Z.; Gao, Z.; Han, L.; Xiao, L. A Novel Approach for In-Situ Preparation of Copper/Graphene Composite with High Hardness and High Electrical Conductivity. *Mater. Lett.* **2022**, *319*, 132219. [[CrossRef](#)]
20. Fan, L.; Yao, W.; Wang, Y. Graphene-Reinforced Copper Matrix Composites: Insights into Interfacial Mechanical Properties of the “Bottom-up” Hybrid Configuration. *Diam. Relat. Mater.* **2021**, *118*, 108519. [[CrossRef](#)]
21. Dong, Z.; Peng, Y.; Zhang, X.; Xiong, D.B. Plasma Assisted Milling Treatment for Improving Mechanical and Electrical Properties of In-Situ Grown Graphene/Copper Composites. *Compos. Commun.* **2021**, *24*, 100619. [[CrossRef](#)]
22. Shi, L.; Liu, M.; Yang, Y.; Liu, R.; Zhang, W.; Zheng, Q.; Ren, Z. Achieving High Strength and Ductility in Copper Matrix Composites with Graphene Network. *Mater. Sci. Eng. A* **2021**, *828*, 142107. [[CrossRef](#)]
23. Zhang, Q.; Qin, Z.; Luo, Q.; Wu, Z.; Liu, L.; Shen, B.; Hu, W. Microstructure and Nanoindentation Behavior of Cu Composites Reinforced with Graphene Nanoplatelets by Electroless Co-Deposition Technique. *Sci. Rep.* **2017**, *7*, 1338. [[CrossRef](#)] [[PubMed](#)]
24. Nayak, D.; Debata, M. Effect of Composition and Milling Time on Mechanical and Wear Performance of Copper–Graphite Composites Processed by Powder Metallurgy Route. *Powder Metall.* **2014**, *57*, 265–273. [[CrossRef](#)]
25. Bata, V.; Pereloma, E.V. An Alternative Physical Explanation of the Hall–Petch Relation. *Acta Mater.* **2004**, *52*, 657–665. [[CrossRef](#)]
26. Yoo, S.C.; Lee, J.; Hong, S.H. Synergistic Outstanding Strengthening Behavior of Graphene/Copper Nanocomposites. *Compos. B Eng.* **2019**, *176*, 107235. [[CrossRef](#)]
27. Arsenault, R.J.; Shi, N. Dislocation Generation Due to Differences between the Coefficients of Thermal Expansion. *Mater. Sci. Eng.* **1986**, *81*, 175–187. [[CrossRef](#)]
28. Yoon, D.; Son, Y.W.; Cheong, H. Negative Thermal Expansion Coefficient of Graphene Measured by Raman Spectroscopy. *Nano Lett.* **2011**, *11*, 3227–3231. [[CrossRef](#)]
29. Yoo, S.J.; Han, S.H.; Kim, W.J. Strength and Strain Hardening of Aluminum Matrix Composites with Randomly Dispersed Nanometer-Length Fragmented Carbon Nanotubes. *Scr. Mater.* **2013**, *68*, 711–714. [[CrossRef](#)]
30. Nardone, V.C.; Strife, J.R. Analysis of the Creep Behavior of Silicon Carbide Whisker Reinforced 2124 Al(T4). *Metall. Trans. A* **1987**, *18*, 109–114. [[CrossRef](#)]

Disclaimer/Publisher’s Note: The statements, opinions and data contained in all publications are solely those of the individual author(s) and contributor(s) and not of MDPI and/or the editor(s). MDPI and/or the editor(s) disclaim responsibility for any injury to people or property resulting from any ideas, methods, instructions or products referred to in the content.